226 nm AlGaN/AlN UV LEDs using p-type Si for hole injection and UV reflection

Dong Liu, Sang June Cho, Jeongpil Park, Jiarui Gong, Jung-Hun Seo, Rafael Dalmau, Deyin Zhao, Kwangeun Kim, Munho Kim, Akhil R. K. Kalapala, John D. Albrecht, Weidong Zhou, Baxter Moody, and Zhenqiang Ma

Citation: Appl. Phys. Lett. **113**, 011111 (2018); doi: 10.1063/1.5038044

View online: https://doi.org/10.1063/1.5038044

View Table of Contents: http://aip.scitation.org/toc/apl/113/1

Published by the American Institute of Physics

226 nm AlGaN/AlN UV LEDs using p-type Si for hole injection and UV reflection

Dong Liu,[1,a)] Sang June Cho,[1,a)] Jeongpil Park,[1,a)] Jiarui Gong,[1] Jung-Hun Seo,[1] Rafael Dalmau,[2] Deyin Zhao,[3] Kwangeun Kim,[1] Munho Kim,[1] Akhil R. K. Kalapala,[3] John D. Albrecht,[4,b)] Weidong Zhou,[3] Baxter Moody,[2] and Zhenqiang Ma[1,b)]
[1]*Department of Electrical and Computer Engineering, University of Wisconsin-Madison, Madison, Wisconsin 53706, USA*
[2]*HexaTech, Inc., 991 Aviation Parkway, Suite 800, Morrisville, North Carolina 27560, USA*
[3]*Department of Electrical Engineering, University of Texas at Arlington, 500 South Cooper Street, Arlington, Texas 76019, USA*
[4]*Department of Electrical and Computer Engineering, Michigan State University, 428 S. Shaw Lane, East Lansing, Michigan 48824, USA*

(Received 30 April 2018; accepted 15 June 2018; published online 5 July 2018)

Deep ultraviolet (UV) light-emitting diodes (LEDs) at a wavelength of 226 nm based on AlGaN/AlN multiple quantum wells using p-type Si as both the hole supplier and the reflective layer are demonstrated. In addition to the description of the hole transport mechanism that allows hole injection from p-type Si into the wide bandgap device, the details of the LED structure which take advantage of the p-type Si layer as a reflective layer to enhance light extraction efficiency (LEE) are elaborated. Fabricated LEDs were characterized both electrically and optically. Owing to the efficient hole injection and enhanced LEE using the p-type Si nanomembranes (NMs), an optical output power of 225 μW was observed at 20 mA continuous current operation (equivalent current density of 15 A/cm^2) without external thermal management. The corresponding external quantum efficiency is 0.2%, higher than any UV LEDs with emission wavelength below 230 nm in the continuous current drive mode. The study demonstrates that adopting p-type Si NMs as both the hole injector and the reflective mirror can enable high-performance UV LEDs with emission wavelengths, output power levels, and efficiencies that were previously inaccessible using conventional p-i-n structures. *Published by AIP Publishing*. https://doi.org/10.1063/1.5038044

Deep ultraviolet (DUV) light sources, especially those at sub-250 nm wavelengths, have attracted increasing interest due to their various applications, such as bio-sensing, medical treatment, high density optical recording, and lithography.[1–5] $Al_xGa_{1-x}N$-based UV light-emitting diodes (LEDs) have advanced to be the most promising solution to achieve deep UV emission due to their wide bandgap energy of up to 6.2 eV (AlN), covering the UV-A (320–400 nm), UV-B (290–320 nm), and UV-C (200–290 nm).[6–16] Although intensive efforts have been invested in development of UV LEDs with high external quantum efficiency (EQE), several critical issues still impede further improvement of the EQE of UV LEDs: (1) growth of high-crystal-quality AlGaN epilayers; (2) lack of conductive *p*-type high-Al-content AlGaN and associated low hole injection efficiency into the active region;[17–21] and (3) compromised light extraction due to absorption of the p-type GaN contact layer, which is commonly adopted to form a conductive ohmic contact.[8,22,23]

Regarding the material growth challenge, AlN substrates were employed to grow AlGaN epilayers with low threading dislocation densities.[24,25] This mitigates defect-related non-radiative recombination that could severely degrade the internal quantum efficiency (IQE). The challenge of p-type doping of AlGaN, which is deemed the most difficult obstacle in the realization of efficient AlGaN-based DUV LEDs, originates from the high Mg acceptor activation energy of approximately 170 meV for GaN, which rises to 630 meV for AlN. In addition to these two challenges, effective light extraction is also essential in order to obtain high EQE. As stated previously, p-type GaN is commonly used as an electrode contact and hole injection layer, since doping p-type AlGaN is inefficient and it is impractical to form good ohmic contacts on the p-type AlGaN at high Al compositions. However, the drawback of using p-type GaN as the contact and hole injector is significant UV absorption of UV photons emitted toward the p-type GaN due to a smaller bandgap energy of p-type GaN compared to the emitted photon energy. To reduce the optical loss and improve light extraction, previous work adopted transparent p-type AlGaN with a high Al composition and a reflective p-type electrode,[12] where the conventional Ni/Au p-type contact metal was substituted with a Ni/Al reflective electrode to increase light extraction efficiency (LEE). However, as the light emission wavelength extends below 240 nm, it is extremely challenging to obtain an effectively doped transparent p-type AlGaN with increasing Al compositions.

To enhance the hole injection of UV LEDs, tunneling junctions were investigated recently: n-AlGaN/InGaN/p-AlGaN,[20,26] metal/InGaN/p-AlGaN,[27] and n-GaN/Al/p-AlGaN[28] (see supplementary material Table I for a summary). However, the use of an n-AlGaN top contact layer was reported to hinder hydrogen diffusion, making it more difficult for Mg activation in the p-AlGaN layer.[29] In addition, the high growth temperature required for AlGaN growth could

[a)]D. Liu, S. J. Cho, J. Park contributed equally to this work.
[b)]Authors to whom correspondence should be addressed: jalbrech@egr.msu.edu and mazq@engr.wisc.edu

cause decomposition of the InGaN interfacial layer and intermixing at elevated temperatures.[27] For the tunneling junction employing metal (Al and Ni) for hole injection,[27] the tunneling barrier height is substantially high due to the large work function difference between metal and p-AlGaN.

Recently, we reported UV LEDs based on $Al_{0.77}Ga_{0.23}N$/AlN multiple quantum wells (MQWs) with a light emission wavelength of 229 nm using a p-type Si nanomembrane (NM) as the hole injection layer.[16] However, the use of 20 nm p-GaN underneath the Si NM imposed significant light absorption for UV photons emitted toward the p-GaN side (opposite to the output through the substrate), which limited the light extraction efficiency and led to a low EQE (0.03%). To reduce the UV photon absorption and make the Si NM function as an effective UV light reflector as reported in this work, the p-type GaN layer between the Si NM and the AlN/$Al_{0.81}Ga_{0.19}N$ MQWs was reduced to 5 nm. With such a layer design, a large fraction of the upward transmitted UV light is reflected and collected from the substrate side. Due to the reduced UV light absorption and thus improved LEE, in addition to the enhanced hole injection using the Si NM, DUV LEDs emitting at a wavelength of 226 nm with a high EQE of 0.2% were demonstrated. The hole transport mechanism for the p-type Si/Al_2O_3/p-type GaN isotype heterojunction can be explained by the energy band alignment and was characterized electrically via both experiments and simulations. Compared to the previous work,[16] more details on the interface tunneling are included to describe the hole injection mechanism. Furthermore, the function of the Si NM on top of the p-type GaN, forming a Si/GaN light reflector, as compared to the GaN/AlGaN case that is commonly used in UV LEDs, was examined. Finally, device performance was characterized by current density–voltage characteristics and electroluminescence (EL) measurements.

The UV LED structure shown schematically in Fig. 1(a) was grown on an AlN substrate by low pressure organometallic vapor phase epitaxy (LP-OMVPE) in a high-temperature reactor. As shown in Fig. 1(a) (i), following an initial 400 nm AlN homoepitaxial layer on the AlN substrate, a Si-doped 600 nm n-$Al_{0.7}Ga_{0.3}N$ contact and electron injection layer was grown prior to the 3-period 3 nm $Al_{0.81}Ga_{0.2}N$/6 nm AlN MQW active region. To minimize the light absorption through the p-type GaN layer, a 5 nm thick p-type GaN layer, serving as the epitaxy termination of AlN/AlGaN MQWs, was grown. It is noted that the p-type GaN is not a hole injector[16] but is used to circumvent the rapid oxidation of the AlN surface.[15] Prior to transferring a 100 nm heavily doped p+ Si single-crystal nanomembrane (NM) with a doping concentration of $5 \times 10^{19}\,cm^{-3}$, a 0.5 nm Al_2O_3 layer as the passivation and highly conductive tunneling layer[16,30] was deposited via atomic layer deposition (ALD) using an Ultratech/Cambridge Nanotech Savannah S200 ALD system, followed by a rapid thermal anneal (RTA) at 500 °C for 5 min to increase the bonding strength between the p-type Si NM and Al_2O_3. A microscopy image of the sample after completion of the Si NM transfer, corresponding to Fig. 1(a) (i), is shown in Fig. 1(b) (i). Figure 1(a) (ii)–(iv) illustrates the fabrication process flow of the LEDs, while Fig. 1(b) (ii)–(iv) shows the corresponding microscopic images of the processing steps. An n-mesa was formed by photolithography image reversal, followed by the etching process of Si and GaN/AlN/AlGaN [Figs. 1(a) (ii) and 1(b) (ii)]. Then, a stack of metals (Ti/Al/Ni/Au, 15/100/50/250 nm) was deposited and annealed at 950 °C for 30 s for cathode formation [Figs. 1(a) (iii) and 1(b) (iii)]. A stack of current spreading layer metals (Ni/Au, 5/10 nm) was deposited and annealed at 550 °C for 1 min followed by contact metal of Ti/Au (10/100 nm). Each device was isolated by etching a trench between devices down to the AlN layer [Figs. 1(a) (iv) and 1(b) (iv)].

A heterojunction consisting of p-type Si/Al_2O_3/p-type GaN for hole tunneling transport was investigated to determine the band alignment and resultant electrical characteristics as shown in Fig. 2. In Fig. 2(a), the test structure is composed of three layers: 100 nm p-type Si (carrier concentration of $5 \times 10^{19}\,cm^{-3}$), 0.5 nm Al_2O_3, and 200 nm p-type GaN (carrier concentration of $5 \times 10^{18}\,cm^{-3}$, assuming 10% of dopant activation ratio). An anode metal was formed on p-type Si and a cathode contact was formed on p-type GaN for electrical measurements, between which the lateral distance was 10 μm. It is known from previous reports that the valence band offset is 1.1 eV between the p-type Si and p-type GaN.[15] The Silvaco® TCA device simulation software was used to simulate the band structures of the isotype heterojunction junction. The simulated band alignment

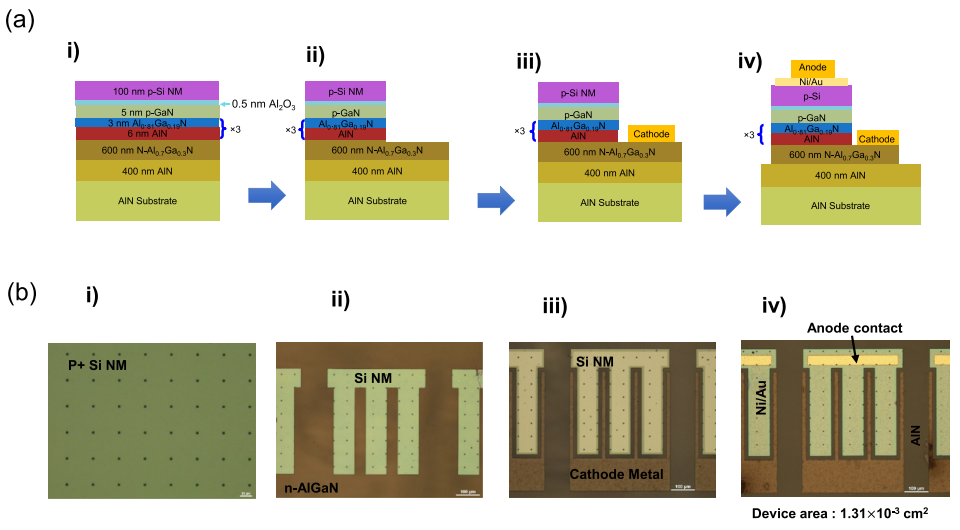

FIG. 1. (a) UV LED fabrication process illustration and (b) the corresponding microscopy images after each step of processing. (i) An epitaxial sample with 0.5 nm Al_2O_3 deposition and 100 nm thick p-type Si NM bonded. (ii) Mesa etch down to the n-type $Al_{0.7}Ga_{0.3}N$ layer. (iii) Cathode. (iv) Anode and device isolation by etching down to the AlN substrate.

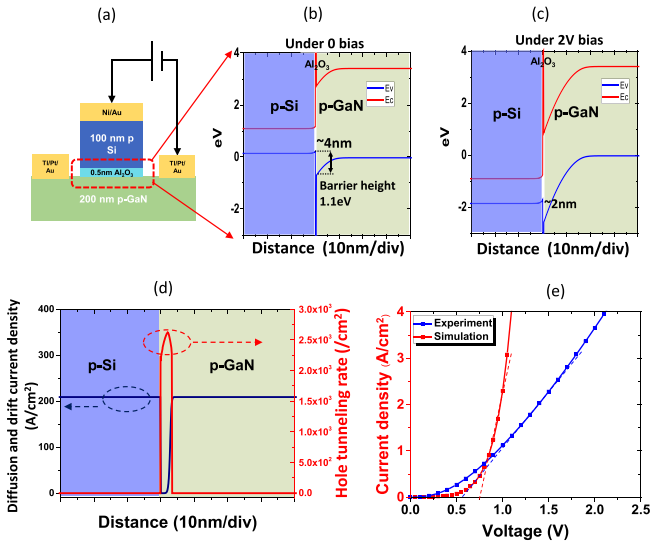

FIG. 2. Heterojunction consisting of p-type Si/Al_2O_3/p-type GaN for hole transport. (a) Cross-sectional illustration of the p-type Si/Al_2O_3/p-type GaN isotype heterojunction test structure. The deposited thickness of Al_2O_3 by ALD is 0.5 nm. The p-type GaN thickness for this testing structure is 200 nm. Simulated band alignment of the p-type Si/Al_2O_3/p-type GaN under (b) thermal equilibrium and (c) positive bias of 2 V applied on Si. (d) Simulated current density and tunneling rate distribution across the p-type Si/Al_2O_3/p-type GaN heterojunction. (e) Simulated and measured electrical I-V characteristics.

including the 0.5 nm Al_2O_3 interfacial layer under thermal equilibrium and 2 V is plotted in Figs. 2(b) and 2(c), respectively. An ~4 nm [Fig. 2(b)] triangular barrier is formed in the valence band by the valence band offset between Si and GaN. As the forward bias is increased, the barrier becomes narrower (down to 2 nm), facilitating the tunneling process for holes from the valence band of p-type Si to that of the p-type GaN layer. Figure 2(d) illustrates the contribution of the hole tunneling current to the total current. As can be seen, the majority current outside the heterojunction interface region is composed of the hole diffusion current or hole drift current, whereas the tunneling-contributed current is dominant across the Al_2O_3 interfacial layer and the valence band tunneling barrier formed in the p-type GaN as a result of the valence band offset. The corresponding simulated and measured current-voltage curves on the linear scale are shown in Fig. 2(e) where turn-on voltages of around 0.75 V and 0.6 V extracted from the simulation and experiments, respectively, were obtained by linear extrapolation. The lower turn-on voltage and higher current at low voltage for the measured vs. simulated data may indicate the existence of interface states with the energy levels within the bandgap near the Fermi-level between Si and GaN, which could result in a higher tunneling rate due to the trap assisted tunneling process.[31] On the other hand, at higher voltages, the slope of the measured J-V curves is less than the simulated slope. This indicates a larger associated series resistance which we attribute to the GaN contact resistance and lateral current spreading resistance within the 200 nm thick GaN in the test device structure [Fig. 2(a)]. It is noted that the series resistances were not taken into account in the simulations.

In the majority of the reported UV LEDs, p-type GaN is used as an electrode contact and hole injection layer instead of p-type AlGaN due to the difficulty in activating p-type dopants in AlGaN. The consequence of adopting p-type GaN is high optical loss for the photons emitted toward the p-type GaN due to the high absorption coefficient of GaN ($\alpha = 3.6 \times 10^5$ cm^{-1} at 226 nm) [Fig. 3(a)]. For this reason, most UV-LEDs employ flip chip packaging for light extraction.[32] In our work, we used p-type Si to bond with 5 nm thick p-type GaN. The impact of the Si/GaN on light extraction efficiency as compared to the GaN/AlGaN case in conventional UV LEDs' contact layer was analyzed. Si is known to be highly absorptive in the UV range due to its small bandgap. In our LED design, due to the extremely short light penetration depth in Si, UV absorption in Si becomes less important. Instead, the UV light is mostly reflected rather than absorbed at the Si surface [Fig. 3(b)]. The complex optical index $(n + ik)$ of Si and $Al_{0.81}Ga_{0.19}N$ over the range of 200 nm–400 nm was fitted based on ellipsometer measurements [supplementary material Figures 1(a) and 1(b)]. For this measurement and fitting, a 200 nm-thick $Al_{0.81}Ga_{0.19}N$ layer was separately grown on a AlN substrate for the optical measurement. The n and k values of GaN were extracted from theoretical dispersion analysis[33] [supplementary material Fig. 1(c)]. The reflectance (R) at 226 nm for normal incidence at the interface between Si ($n_{Si} = 1.43 + 3.37i$) and GaN ($n_{GaN} = 2.78 + 0.65i$) is 24%, whereas the reflectance is only 1% between GaN and AlGaN ($n_{AlGaN} = 2.40 + 0.31i$) for conventional UV LED structures employing a top p-type GaN contact layer. Figure 3(b) depicts

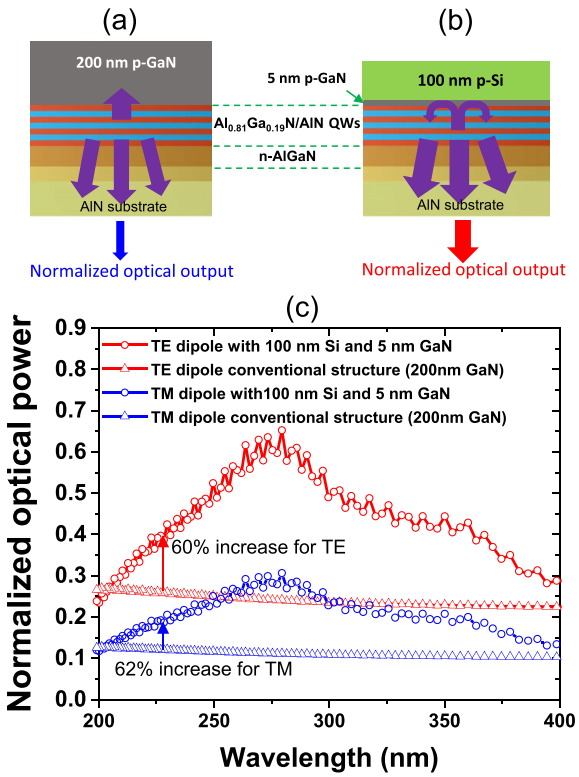

FIG. 3. Light extraction efficiency (LEE) for the two LED structures. (a) Conventional LED structure with 200 nm p-type GaN on top of MQWs as the contact layer. (b) LED structure with p-type Si on top of 5 nm p-type GaN. (c) Simulated light transmission proportion collected from the bottom (AlN substrate side) of the two structures for TE (red) and TM (blue) dipoles, respectively. Compared with the conventional structure with the 200 nm p-GaN contact layer, the proposed structure exhibits 60% and 62% increase of light output power collected from the AlN substrate side for TE and TM dipoles, respectively.

that due to the large index difference between the Si NM and GaN, the Si NM significantly enhanced the UV light reflection when the light propagated towards the interface of GaN/Si as compared to AlGaN/GaN.

To comprehensively evaluate the LEE enhancement by the Si NM, the reflectance of both TE and TM polarization modes of the UV light that was emitted from the MQWs was considered. The finite-difference time-domain method (FDTD) was used to simulate the light propagation path, accounting for the light emitted from TE and TM dipoles within the QW region (see supplementary material Fig. 2 for detailed simulation structure setup) for the conventional UV LED [Fig. 3(a)] and the p-type Si UV LED [Fig. 3(b)]. Figure 3(c) shows the quantitative comparison of the normalized optical output emission from the AlN substrate side between the two LEDs for TE and TM dipoles, respectively. It is shown that compared with the conventional structure with a 200 nm p-GaN contact layer, the proposed structure exhibits 60% and 62% increase of light output power collected from the AlN substrate side for TE and TM dipoles, respectively. The appearance of ripples for the TE dipole light output in the proposed structure is attributed to the resonance effect due to the enhanced reflectivity of the top layer. To clearly visualize the reflector effect of the p-Si NM layer, the light propagation and reflection behaviors for each dipole in the two types of structures were recorded in movies as shown in supplementary material Fig. 3 [(a): TE dipole in the structure of Fig. 3(a) (Multimedia view); (b): TE dipole in the structure of Fig. 3(b) (Multimedia view); (c): TM dipole in the structure of Fig. 3(a) (Multimedia view); (d): TM dipole in the structure of Fig. 3(b) (Multimedia view)]. It is noted that the light transmitted in the upward (p-type side) direction is negligible as it is either reflected or absorbed by the p-type Si or p-type GaN. Under this consideration, the normalized optical output emitted from the substrate is considered equivalent to LEE. Thus, a 60%–62% of LEE improvement was expected by employing the p-type Si depending on the accurate proportion between the TE and TM emission, which is sensitive to various factors including strain in the quantum well, Al composition in the quantum barrier, and thickness of the wells.[34] Overall, the p-type Si NM on top of the UV LED epitaxial structure indeed serves as a UV reflection layer, which we subsequently used to greatly enhance the UV light extraction from the thinned AlN substrate side.

The electrical performances of the LEDs including current density-voltage and EL measurements are shown in Figs. 4(a) and 4(b), respectively. It can be seen from the linear scale plot that the LED has rectifying characteristics and a turn-on voltage of about 11 V. The relatively large turn-on voltage resulted from the large valence band barrier between GaN and the first quantum barrier (AlN) and also from the non-ohmic metal contact made on the n-type $Al_{0.7}Ga_{0.3}N$ layer (see supplementary material Fig. 3 for details). On the other hand, the low reverse current density revealed on the log scale indicates the absence of a significant leakage path, either through surface recombination or defects at the interface between Si and GaN.

The EL spectrum and optical power measurements were performed by coupling LED emission into a 6-in. diameter integrating sphere of a Gooch and Housego OL 770-LED calibrated spectroradiometer. Electrical power was supplied in the constant current mode, and the temperature was not controlled. The measured EL spectrum on the linear scale

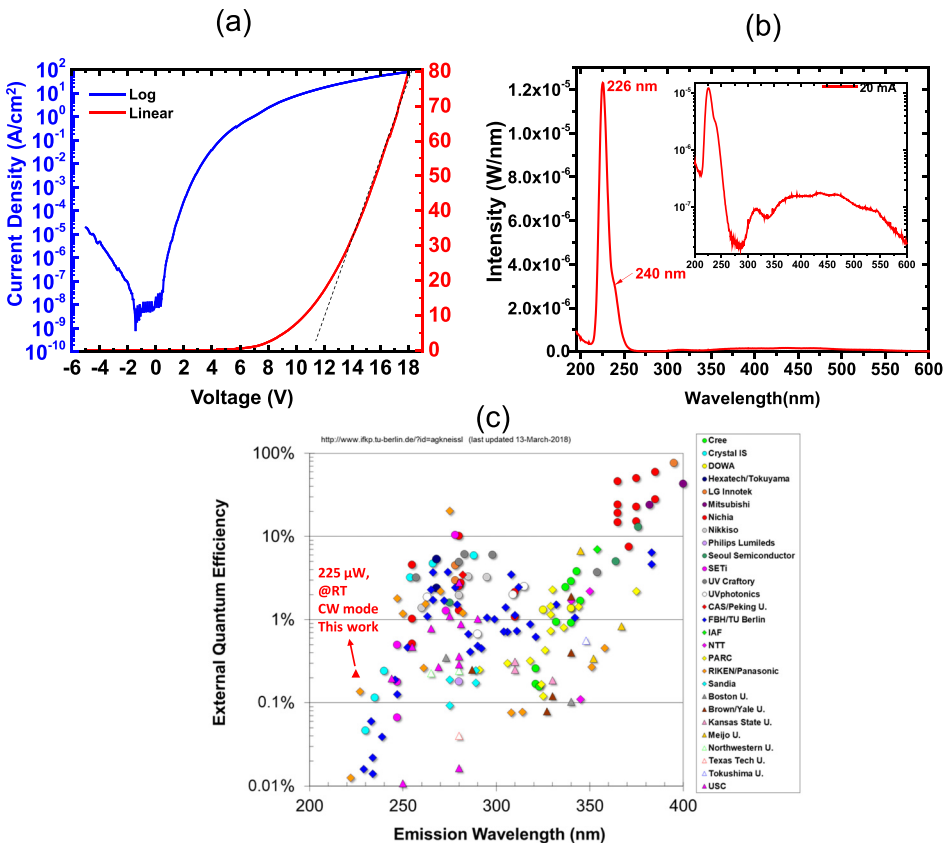

FIG. 4. (a) Measured current density-voltage characteristics of a typical LED on the linear and the log scale. (b) EL spectra under 20 mA driving current with a constant drive current operation mode. The inset depicts the corresponding spectra on the log scale. (c) EQE comparison with reported AlGaN-, InAlGaN-, and InGaN-based LEDs emitting in the UV spectral region[35] (original figure courtesy of Michael Kneissl, Technische Universität Berlin) (RT: room temperature; CW: continuous wave).

under a constant drive current of 20 mA is shown in Fig. 4(b), and the inset plots the corresponding log scale spectrum. The 226 nm peak radiating from the MQWs is dominant, with one discernible weaker feature at around 240 nm, which is speculated to be emitted from the n-$Al_{0.7}Ga_{0.3}N$ layer. The weak light emission over the 300–600 nm wavelength range has two possible origins. One is electron overflow into the very thin p-GaN layer and the resultant recombination therein. The other is reabsorption of the QW light emission due to the smaller bandgap of GaN. The relatively suppressed 300–600 nm spectrum compared to our previous report,[16] where a thicker p-GaN of 20 nm was used, may serve as proof that the GaN layer is responsible for the 300–600 nm light emission.

Moreover, the optical output power versus current was measured. A power intensity of 225 μW was obtained at 20 mA with an equivalent current density of 15 A/cm^2, and the corresponding external quantum efficiency (EQE) was calculated to be 0.2%. This EQE value is higher than any UV LEDs in the comparable wavelength range,[35] as shown in Fig. 4(c). It is noted that the EQE could be further improved by additional thinning of the AlN substrate, which induces substantial absorption due to point defects in the substrate,[36] and by incorporating light extraction patterning. From our device testing, no reliability issues were observed due to the addition of the Si layer.

In summary, by using p-type Si as the hole injector and UV light reflector to enhance light extraction, 226 nm UV LEDs based on AlN/$Al_{0.81}Ga_{0.19}N$ epitaxial MQWs heterostructures on bulk AlN substrates were demonstrated. At a current injection density of 15 A/cm^2, an output optical power of 225 μW with a corresponding EQE value of 0.2% under continuous current and room temperature operation was measured. This work suggests that using Si NM as the hole injector and optical reflector for high Al composition-based LEDs can be a practical route toward high-performance DUV LEDs for short wavelengths and high efficiency.

See supplementary material for (1) summary of reported UV LEDs employing tunneling junctions along with performance comparison with this work; (2) optical properties (n, k) for Si, GaN, and $Al_{0.81}Ga_{0.19}N$; (3) optical simulation for light extraction efficiency (LEE); (4) movie files showing light propagation and reflection behaviors for TE and TM dipoles in the two types of structures as shown in Figs. 3(a) and 3(b); (5) circular transmission line method (CTLM) measurements for n-type $Al_{0.7}Ga_{0.3}N$ metal contact.

This work was supported by the Defense Advanced Research Projects Agency (DARPA) under Grant No. HR0011-15-2-0002. The program manager is Dr. Daniel Green.

[1]J. Simon, V. Protasenko, C. Lian, H. Xing, and D. Jena, Science **327**, 60 (2010).
[2]J. Verma, P. K. Kandaswamy, V. Protasenko, A. Verma, H. Xing, and D. Jena, Appl. Phys. Lett. **102**, 041103 (2013).
[3]Y. Taniyasu and M. Kasu, Appl. Phys. Lett. **99**, 251112 (2011).
[4]J. Verma, S. M. Islam, V. Protasenko, P. K. Kandaswamy, H. Xing, and D. Jena, Appl. Phys. Lett. **104**, 021105 (2014).
[5]S. M. Islam, K. Lee, J. Verma, V. Protasenko, S. Rouvimov, S. Bharadwaj, H. Xing, and D. Jena, Appl. Phys. Lett. **110**, 041108 (2017).
[6]J. P. Zhang, M. A. Khan, W. H. Sun, H. M. Wang, C. Q. Chen, Q. Fareed, E. Kuokstis, and J. W. Yang, Appl. Phys. Lett. **81**, 4392 (2002).
[7]Y. Taniyasu, M. Kasu, and T. Makimoto, Nature **441**, 325 (2006).
[8]J. S. Park, J. K. Kim, J. Cho, and T.-Y. Seonga, ECS J. Solid State Sci. Technol. **6**, Q42 (2017).
[9]H. Hirayama, N. Noguchi, T. Yatabe, and N. Kamata, Appl. Phys. Express **1**, 051101 (2008).
[10]H. Hirayama, N. Noguchi, and N. Kamata, Appl. Phys. Express **3**, 032102 (2010).
[11]T. Nishida, H. Saito, and N. Kobayashi, Appl. Phys. Lett. **79**, 711 (2001).
[12]H. Hirayama, N. Maeda, S. Fujikawa, S. Toyoda, and N. Kamata, Jpn. J. Appl. Phys., Part 1 **53**, 100209 (2014).
[13]J. Han, M. H. Crawford, R. J. Shul, J. J. Figiel, M. Banas, L. Zhang, Y. K. Song, H. Zhou, and A. V. Nurmikko, Appl. Phys. Lett. **73**, 1688 (1998).
[14]C. Pernot, S. Fukahori, T. Inazu, T. Fujita, M. Kim, Y. Nagasawa, A. Hirano, M. Ippommatsu, M. Iwaya, S. Kamiyama, I. Akasaki, and H. Amano, Phys. Status Solidi A **208**, 1594 (2011).
[15]S. J. Cho, D. Liu, J.-H. Seo, R. Dalmau, K. Kim, J. Park, D. Zhao, X. Yin, Y. H. Jung, I.-K. Lee, J. D. Albrecht, W. Zhou, B. Moody, and Z. Ma, preprint arXiv:1707.04223 (2017).
[16]D. Liu, S. J. Cho, J. Park, J.-H. Seo, R. Dalmau, D. Zhao, K. Kim, M. Kim, I.-K. Lee, J. D. Albrecht, W. Zhou, B. Moody, and Z. Ma, "229 nm UV LEDs on aluminum nitride single crystal substrates using p-type silicon for increased hole injection," Appl. Phys. Lett. **112**, 081101 (2018).
[17]O. Ambacher, B. Foutz, J. Smart, J. R. Shealy, N. G. Weimann, K. Chu, M. Murphy, A. J. Sierakowski, W. J. Schaff, L. F. Eastman, R. Dimitrov, A. Mitchell, and M. Stutzmann, J. Appl. Phys. **87**, 334 (2000).
[18]Z. Peng, L. Shi-Bin, Y. Hong-Ping, W. Zhi-Ming, C. Zhi, and J. Ya-Dong, Chin. Phys. Lett. **31**, 118102 (2014).
[19]S. M. Sadaf, S. Zhao, Y. Wu, Y. H. Ra, X. Liu, S. Vanka, and Z. Mi, Nano Lett. **17**, 1212 (2017).
[20]Y. Zhang, S. Krishnamoorthy, J. M. Johnson, F. Akyol, A. Allerman, M. W. Moseley, A. Armstrong, J. Hwang, and S. Rajan, Appl. Phys. Lett. **106**, 141103 (2015).
[21]A. G. Sarwar, B. J. May, J. I. Deitz, T. J. Grassman, D. W. McComb, and R. C. Myers, Appl. Phys. Lett. **107**, 101103 (2015).
[22]J. W. Lee, D. Y. Kim, J. H. Park, E. F. Schubert, J. Kim, J. Lee, Y.-I. Kim, Y. Park, and J. K. Kim, Sci. Rep. **6**, 22537 (2016).
[23]H.-Y. Ryu, I.-G. Choi, H.-S. Choi, and J.-I. Shim, Appl. Phys. Express **6**, 062101 (2013).
[24]R. Dalmau, B. Moody, R. Schlesser, S. Mita, J. Xie, M. Feneberg, B. Neuschl, K. Thonke, R. Collazo, and A. Rice, J. Electrochem. Soc. **158**, H530 (2011).
[25]T. Wunderer, C. Chua, J. Northrup, Z. Yang, N. Johnson, M. Kneissl, G. Garrett, H. Shen, M. Wraback, B. Moody, H. S. Craft, R. Schlesser, R. F. Dalmau, and Z. Sitar, Phys. Status Solidi C **9**, 822 (2012).
[26]Y. Zhang, Z. J. Eddine, F. Akyol, S. Bajaj, J. M. Johnson, G. Calderon, A. A. Allerman, M. W. Moseley, A. M. Armstrong, J. Hwang, and S. Rajan, Appl. Phys. Lett. **112**, 071107 (2018).
[27]Y. Zhang, S. Krishnamoorthy, F. Akyol, J. M. Johnson, A. A. Allerman, M. W. Moseley, A. M. Armstrong, J. Hwang, and S. Rajan, Appl. Phys. Lett. **111**, 051104 (2017).
[28]S. Zhao, S. M. Sadaf, S. Vanka, Y. Wang, R. Rashid, and Z. Mi, Appl. Phys. Lett. **109**, 201106 (2016).
[29]Y. Kuwano, M. Kaga, T. Morita, K. Yamashita, K. Yagi, M. Iwaya, T. Takeuchi, S. Kamiyama, and I. Akasaki, Jpn. J. Appl. Phys., Part 1 **52**(8S), 08JK12 (2013).
[30]Z. Ma and J.-H. Seo, "Lattice mismatched heterojunction structures and devices made therefrom," U.S. patent 8,866,154 (21 October 2014).
[31]S. M. Sze and K. K. Ng, *Physics of Semiconductor Devices* (Wiley-Interscience, 2006).
[32]A. Khan, K. Balakrishnan, and T. Katona, Nat. Photonics **2**, 77–84 (2008).
[33]T. Kawashima, H. Yoshikawa, and S. Adachi, "Optical properties of hexagonal GaN," J. Appl. Phys. **82**, 3528–3535 (1997).
[34]J. E. Northrup, C. L. Chua, Z. Yang, T. Wunderer, M. Kneissl, N. M. Johnson, and T. Kolbe, Appl. Phys. Lett. **100**, 021101 (2012).
[35]M. Kneissl, see https://www.ifkp.tu-berlin.de/?id=agkneissl for Curriculum Vitae (last updated 13 March, 2018).
[36]R. Collazo, J. Xie, B. E. Gaddy, Z. Bryan, R. Kirste, M. Hoffmann, R. Dalmau, B. Moody, Y. Kumagai, and T. Nagashima, Appl. Phys. Lett. **100**, 191914 (2012).